Available online at www.sciencedirect.com
ScienceDirect
Organisms, Diversity & Evolution 7 (2007) 33–51
ORGANISMS DIVERSITY & EVOLUTION
www.elsevier.de/ode

Phylogenetic analysis of Remipedia (Crustacea)

Stefan Koenemann[a,*], Frederick R. Schram[b], Mario Hönemann[a], Thomas M. Iliffe[c]

[a]*Institute for Animal Ecology and Cell Biology, University of Veterinary Medicine Hannover, Bünteweg 17d, 30559 Hannover, Germany*
[b]*Institute of Biodiversity and Ecosystem Dynamics, University of Amsterdam, Mauritskade 57, 1092 AD Amsterdam, The Netherlands*
[c]*Department of Marine Biology, Texas A&M University at Galveston, Galveston, TX 77553-1675, USA*

Received 25 January 2006; accepted 6 July 2006

Abstract

We present a cladistic analysis of the crustacean class Remipedia, including all 17 extant species currently assigned to the order Nectiopoda, with the Carboniferous fossil *Tesnusocaris* serving as an outgroup. We applied different methodological approaches and coding options to a basic matrix composed of 26 morphological characters. Our analyses strongly support monophyly of the Godzilliidae and affirm justification of the family Micropacteridae. However, the present taxonomic structure within the Speleonectidae is partly incompatible with our results, and we cannot exclude that the family is paraphyletic.

Keywords: Remipedia; Micropacteridae; *Tesnusocaris*; Phylogenetic analysis

Introduction

Among the diversity of crustacean body plans, the class Remipedia is indeed a 'class apart' distinguished by a set of unique features. Remipedes are hermaphroditic crustaceans that occur exclusively in subterranean marine environments. The head region of these stygobionts is armed with three pairs of powerful, raptorial limbs. However, it is their long, homonomously segmented trunk bearing biramous, paddle-shaped appendages (Fig. 1A) that has led to the prevalent view that remipedes are primitive crustaceans, although this assumption has not yet been verified or falsified convincingly. For example, the results of our ongoing phylogenetic reconstruction of extant and fossil crustaceomorph arthropods casts doubt about remipedes as 'basal' crustaceans (Schram and Koenemann 2004). Recent comparative studies of cerebral structures in arthropods suggest a sister-group relationship between Malacostraca and Remipedia (Fanenbruck et al. 2004; Harzsch 2004).

It certainly adds to the fascination of remipede crustaceans that this group is relatively new to science. The first remipede was discovered in an anchialine cave on the Bahamas Islands (Yager 1981). Between 1980 and 2005, 17 more remipedes have been discovered, including a new family (Koenemann et al. 2007). At present, the order Nectiopoda is composed of three families:

(1) Godzilliidae Schram et al., 1986, with three monotypic genera;

*Corresponding author.
E-mail address: stefan.koenemann@tiho-hannover.de (S. Koenemann).

1439-6092/$ - see front matter © 2006 Gesellschaft für Biologische Systematik. Published by Elsevier GmbH. All rights reserved.
doi:10.1016/j.ode.2006.07.001

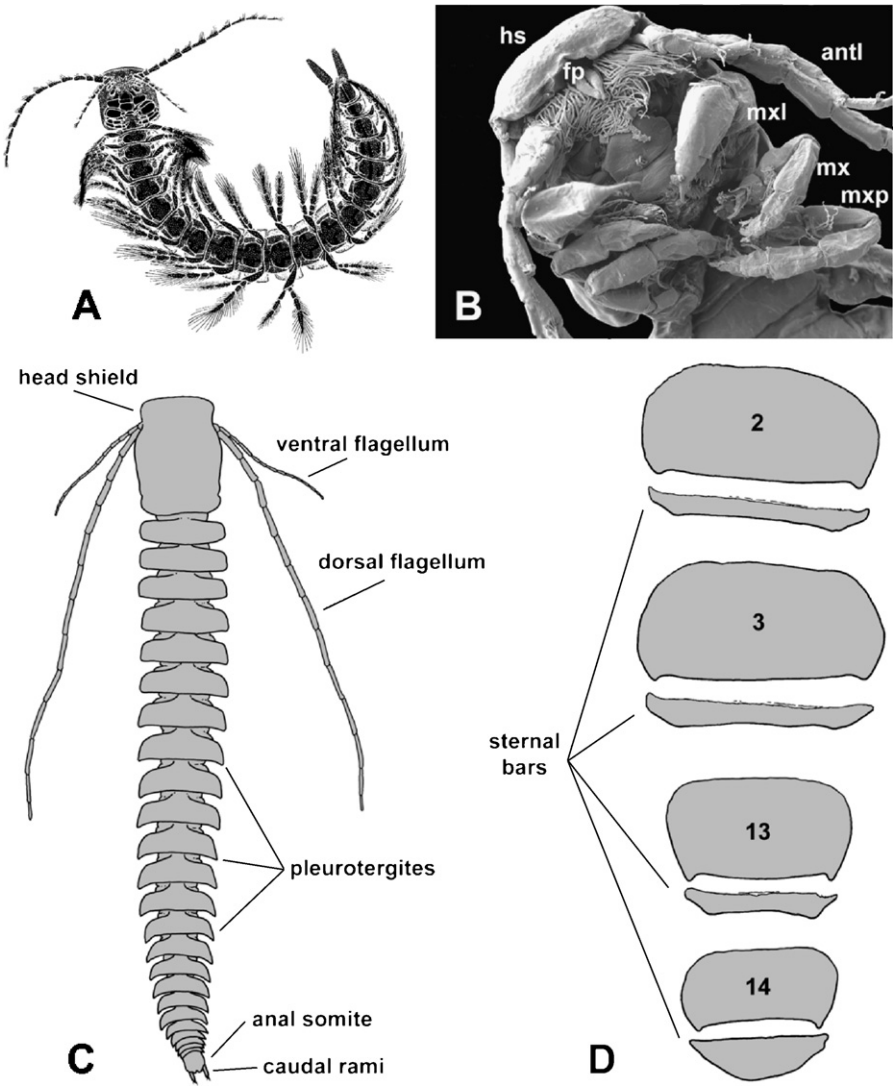

Fig. 1. (A) Habitus drawing of *Speleonectes ondinae,* ventral view (from Schram et al. 1986). (B) Head of *S. tanumekes*, ventral view; antl = antennule, fp = frontal process, hs = head shield, mx = maxilla, mxl = maxillule, mxp = maxilliped (modified after Koenemann et al. 2003). (C) Head and trunk of *S. parabenjamini*, dorsal view. (D) Sternites and sternal bars of *S. parabenjamini*; numbers indicate trunk segments (modified after Koenemann et al. 2003).

(2) Speleonectidae Yager, 1981, comprising nine species in three genera;
(3) Micropacteridae Koenemann et al., 2007, with a single genus and species.

All currently known taxa occur in subtropical belts. The Remipedia exhibit a classical disjunct distribution, with a main cluster of taxa in the greater Caribbean region, an isolated species on Lanzarote and another in Western Australia. This disjunct pattern is believed to reflect a Tethyan origin of this group of crustaceans (Schram 1983; Humphreys 1993; Yager and Humphreys 1996). Therefore, a phylogenetic analysis of the Remipedia seemed particularly desirable to gain insight into the biogeographic history of the group.

The necessity for a phylogenetic analysis of Remipedia became even more evident after a number of recent discoveries of new taxa from the Bahamas. These included three species of speleonectids (Koenemann et al. 2003), the genus *Kaloketos* (Koenemann et al. 2004) and, in particular, the new family Micropacteridae (Koenemann et al. 2007). The recognition of new taxa revealed several critical inconsistencies of diagnoses at and below the family level. Therefore, investigating the phylogenetic relationships within Remipedia has become an important objective towards establishing a stable taxonomy.

In this paper, we present the results of a phylogenetic analysis comprising all 17 currently known species of the remipede order Nectiopoda. Our investigation is based

on 26 morphological characters and includes the fossil remipede *Tesnusocaris* as an outgroup.

Definitions of morphological terms

For a convenient discussion of cephalic appendages we need short, unambiguous terms to refer to the proximal and distal regions of the remipede maxillules, maxillae and maxillipeds. Since the maxillae and maxillipeds in godzilliids show a striking resemblance to the subchelate gnathopods in malacostracans (e.g. Amphipoda), one may be tempted to apply malacostracan terminology, i.e. 'propodus' and 'dactylus', to the raptorial limbs of remipedes. However, we need to be cautious with homologizing particular components of remipede mouthparts with cephalic or thoracic appendages of other groups based merely on function or similarity of form. Of course, this applies to arthropod limb morphology in general. Moreover, malacostracan gnathopods are seven-segmented (not counting the nail), while the prehensile limbs in remipedes are composed of seven to nine segments (see also Discussion).

Therefore, we partly adopted the morphological nomenclature from Koenemann et al. (2003). The terms lacertus and brachium are newly introduced by Koenemann et al. (2007). In addition, we use the following unmistakable terms to define morphological structures in Remipedia.

Sectorization. In most nectiopod remipedes, individual segments of maxillae and maxillipeds form functional units that can differ distinctly in size and shape. In these 'sectorized' appendages, the segment proximal to the elbow (the lacertus) is typically much longer and wider than the segments distal to the elbow (the brachium). Moreover, in advanced stages of sectorization, the brachium exhibits varying degrees of segment fusion (Fig. 2C, D). If sectorization is completely lacking, the individual segments of the lacertus and the brachium are subequal in width as well as in length, for example in *Tesnusocaris* (Fig. 2B). The prehensile limbs of some speleonectids show intermediate degrees of sectorization, with weakly expanded and/or shortened segments (Fig. 2A).

Heteromorphic. This term refers to sternal bars that are differently shaped on some trunk sternites. The male gonopores of the hermaphroditic remipedes are located on trunk segment 14. In some taxa, the sternal bars on this segment are modified into enlarged, flap-like structures (Fig. 1D). However, heteromorphy can also occur as a serial modification; in some remipedes, for example, sternal bars 1–14 can have a concave distal margin, while those on the posterior trunk are convex.

Isomorphic. Isomorphic sternal bars are typically sublinear (with parallel margins) and subequal, thus not modified on trunk segment 14 or any other trunk segment. We also use the terms 'isomorphic' and 'heteromorphic' to distinguish between different morphological types of setae.

Phylogenetic analysis of Remipedia

Methodology

Choice of ingroup taxa – the order Nectiopoda

We included in our analysis all remipedes currently assigned to the order Nectiopoda (see also Appendices A and B). The traditional arrangement of these taxa is as follows:

(1) Family Speleonectidae, composed of 13 species in four genera: *Cryptocorynetes haptodiscus* Yager, 1987a; *Kaloketos pilosus* Koenemann et al., 2004; *Lasionectes entrichoma* Yager & Schram, 1986; *L. exleyi* Yager & Humphreys, 1996; *Speleonectes benjamini* Yager, 1987a; *S. epilimnius* Yager & Carpenter, 1999; *S. gironensis* Yager, 1994; *S. lucayensis* Yager, 1981; *S. ondinae* (Garcia-Valdecasas, 1984); *S. tulumensis* Yager, 1987b; *S. tanumekes* Koenemann et al., 2003; *S. parabenjamini* Koenemann et al., 2003; *S. minnsi* Koenemann et al., 2003.

(2) Family Godzilliidae, with three species in monotypic genera: *Godzilliognomus frondosus* Yager, 1989; *Godzillius robustus* Schram et al., 1986; *Pleomothra apletocheles* Yager, 1989.

(3) Family Micropacteridae, with the single genus and species *Micropacter yagerae* Koenemann et al., 2007.

Outgroup taxon – a remipede fossil of the order Enantiopoda

The primary goal of this study was to analyze the phylogenetic relationships within the Nectiopoda, and in particular, to determine the status of the new family Micropacteridae within the order. In this case, the ideal outgroup taxon would be the closest stem-group relative to the most basal nectiopod. We consider the Carboniferous fossil *Tesnusocaris goldichi* Brooks, 1955 an appropriate choice of outgroup taxon. Its position as a sister group to the Remipedia was repeatedly and robustly confirmed in more comprehensive analyses investigating the position of remipedes within the Crustacea s. lat. (Schram and Hof 1997; Schram and Koenemann 2004). *Tesnusocaris*, from the Tesnus Formation (Upper Mississippian/Lower Pennsylvanian) in Texas, was redescribed by Emerson and Schram (1991). Although some aspects of their reconstructions seem questionable, in our analyses we have accepted their interpretations, in particular of the cephalic appendages, at face value and scored our characters in accordance with the redescription. The other fossil

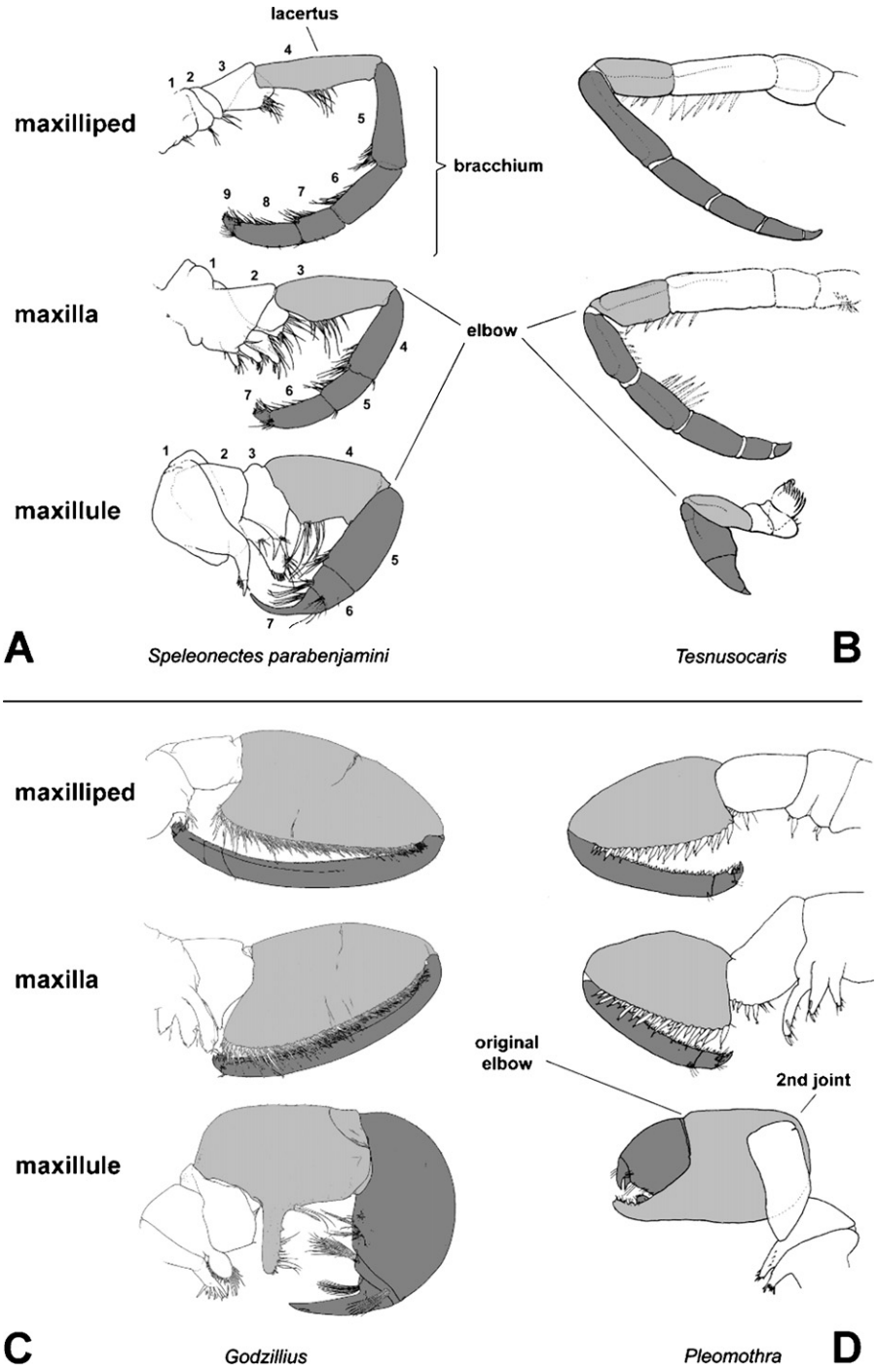

Fig. 2. Comparison of prehensile limbs in enantiopods and nectiopods. (A) *Speleonectes parabenjamini* (Nectiopoda, Speleonectidae; modified after Koenemann et al. 2003). (B) *Tesnusocaris goldichi* (Enantiopoda; modified after Emerson and Schram 1991). (C) *Godzillius robustus* (Nectiopoda, Godzilliidae; modified after Schram et al. 1986). (D) *Pleomothra apletocheles* (Nectiopoda, Godzilliidae; modified after Yager 1989). Light shading: lacertus; dark shading: brachium (see text in ''Definitions of morphological terms''). Numbers indicate individual limb segments. Limbs of *Pleomothra* not drawn to scale; maxillule is much larger than maxilla and maxilliped. Note the fusion of segments in brachia of maxillae and maxillipeds of the two godzilliids.

enantiopod remipede, *Cryptocaris hootchi* Schram, 1974 from the Mazon Creek Formation (Middle Pennsylvanian) in Illinois, is too insufficiently known to be included in this analysis.

Parsimony analysis

We used PAUP* version 4.0b10 to conduct a parsimony analysis of the 17 currently known species of Remipedia, with *Tesnusocaris goldichi* designated as

the outgroup taxon. Our initial data matrix is composed of 26 morphological features, of which four were binary and 22 multi-state characters (Appendix A). Characters were scored based on examinations of collection material and taxonomic descriptions gleaned from the literature.

Since we were particularly interested in evaluating the phylogenetic position of the Micropacteridae, we rescored some of the character states that represent crucial diagnostic features of this newly described nectiopod family (Koenemann et al. 2007). In total, we changed five character states that allowed alternative interpretations of peculiar autapomorphic features in *Micropacter*. The resulting, alternative matrix was analyzed using the same options and parameters (described below) applied to the initial matrix. We do not have a preference for either one of the two matrices, and will refer to them as matrix A and matrix B, or accordingly, analysis A and B, in the following text. A detailed discussion of alternative interpretations of character states is given in the section ''Characters and character states''.

The data (both matrices) were analyzed using a branch-and-bound search, including only parsimony-informative characters. We chose the following general parsimony options: optimality criterion = parsimony; multi-state taxa interpreted as uncertainty; character-state optimization = accelerated transformation (ACCTRAN). To improve computing time, we first conducted a heuristic search for an approximation of the upper bound, which was used for the subsequent branch-and-bound search (settings: stepwise addition; addition sequence = random; number of replicates = 30; number of trees held at each step = 7; branch swapping algorithm = TBR; steepest descent = on; zero-length branches not collapsed; ''MulTrees'' option in effect; topological constraints not enforced).

We chose two alternative coding designs to compare the behavior of character transformations under constrained and unconstrained conditions. For an initial, unconstrained analysis, all characters were left unordered and unweighted. Subsequently, a strict consensus tree was evaluated tracing the transformation of characters among taxa. Based on these results, we applied constraints to characters that were subjected to presumably improbable reversals or parallelisms (constrained analysis). For example, it is very unlikely, or 'non-parsimonious', that the fused, horseshoe-type of claw found in most species of *Speleonectes* evolved back into a few, long free denticles as featured in the unconstrained analyses (see Fig. 3). In this and similar instances, step matrices were designed to constrain improbable character transformations.

Reweighting characters

We applied PAUP's ''reweight characters''option to the constrained and unconstrained versions of matrices A and B. Characters were reweighted by the maximum value of rescaled consistency indices, using the same branch-and-bound settings (described above).

Support values – decay indices and bootstrap analyses

To evaluate the robustness of each of the four trees obtained from the parsimony analyses, we used the bootstrap method available in PAUP. However, it did not seem feasible to conduct bootstrap analyses using the branch-and-bound method, since computing time turned out to be intolerably long, even on a G5 Dual PowerMac. Therefore, we chose a heuristic search for the bootstrap analyses of both matrices (1000 replicates; optimality criterion = parsimony; addition sequence = random; number of replicates = 10; random trees used as starting point; number of trees held at each step during stepwise addition = 7; branch-swapping algorithm = TBR; zero-length branches not collapsed; ''MulTrees'' option in effect; topological constraints not enforced; steepest descent option not in effect).

In addition to bootstrapping, we calculated decay indices (Bremer support) for all maximum parsimony trees (MPTs) using the program TreeRot.

Characters and character states

As mentioned above, the five alternative characters and states for the new family Micropacteridae resulted in two matrices. The following section describes the characters and states of matrix A. Character states encoded differently in matrix B are also described within this section. If not indicated otherwise, characters were left unordered in the second, constrained analysis.

Character numbers are in consecutive order and correspond with numerals in the header row of the matrix (Appendix A) as well as with state changes mapped onto two trees (Figs. 4 and 6).

To optimize computing time of the branch-and-bound searches, we decided to exclude all characters that were uninformative for the parsimony analysis. However, we think that some of the excluded characters may contain significant phylogenetic signal and, thus, deserve further investigation, for example detailed morphological studies of head shields, SEM analyses of mandibular processes, setae on all appendages, and, in particular, the gonopores.

1. Frontal filaments, medial process
   - 0: short
   - 1: long
   - 2: very long, bifurcate

The frontal filaments in nectiopods are small, bifurcate paired processes located on the ventroanterior part of the cephalon, slightly anterior to the antennules (Fig. 1B). They may be sensory organs, but their exact

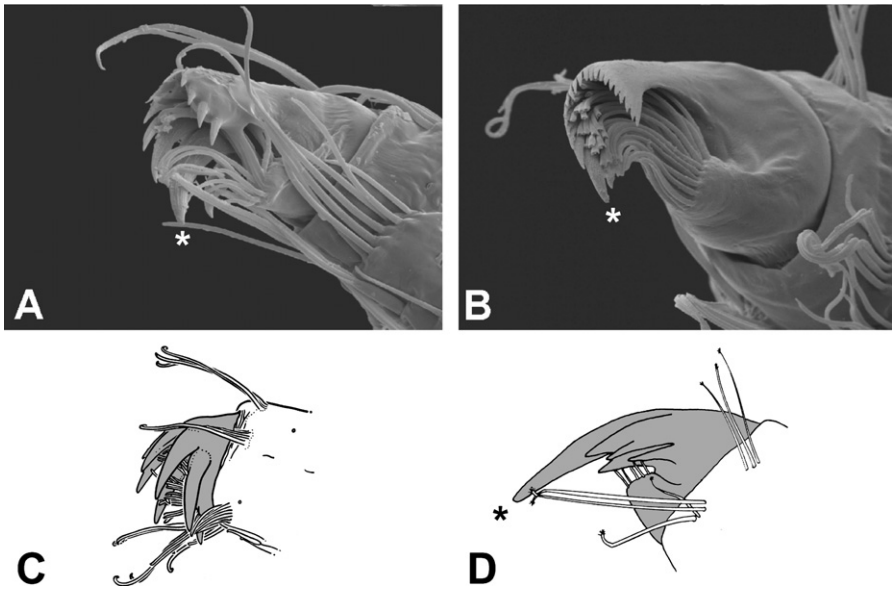

Fig. 3. Claw types of maxillae and maxillipeds in Nectiopoda. (A) Horseshoe-type claw of *Speleonectes parabenjamini* (modified after Koenemann et al. 2003). (B) Horseshoe-type claw of *S. tanumekes* (modified after Koenemann et al. 2003). (C) Grappling hook-type claw of *Godzillius robustus* (modified after Schram et al. 1986). (D) Longfinger-type claw of *Pleomothra apletocheles* (modified after Yager 1989). Asterisk indicates dominant denticle.

function is unknown. The midmedial processes of these filaments can be short, not reaching half the distance from their base to the apex of the main filament (state 0). Long processes are as long as the main filament (state 1). In *Micropacter*, the midmedial processes are bifurcate and much longer than the main filament (state 2).

2. Lateral margins of pleurotergites
    0: all angled
    1: some pointed or angled
    2: all distinctly pointed
    3: completely reduced

In most nectiopod remipedes, the lateral pleurites, or pleurotergites, extend well beyond the width of the trunk (state 0; see Fig. 1A, C). In the three godzilliid genera, all pleurotergites are distinctly pointed (state 2), while the Speleonectidae have pointed pleurites only in the posterior part of the trunk (state 1). *Micropacter*, by contrast, shows a distinct reduction of the pleurotergites, by which the trunk appears comparatively slender (state 3).

3. Sternal plates
    0: simple
    1: with pointed posterolateral corners

State 0 defines all taxa that have simple-shaped sternal plates, while *S. benjamini*, *S. parabenjamini* and *Kaloketos* exhibit pointed posterolateral corners of the sternal plates (state 1; see Fig. 1D).

4. Sternal bars
    0: isomorphic
    1: heteromorphic
    2: heteromorphic but reduced
    MATRIX B: state 2 deleted

Sternal bars are transverse, cuticular ridges along the posterior margins of trunk sternites. State 0 is the condition in all taxa that have similarly shaped, straight sternal bars throughout the trunk (see "Definitions of morphological terms"). In some taxa, however, the shape of the sternal bars varies along the trunk: while the sternal bars on anterior segments are narrow and sometimes slightly concave, the posterior trunk bears flap-like bars (Fig. 1D). The abrupt transition between these two forms is demarcated by trunk segment 14, where the male gonopores are located. In all taxa with heteromorphic sternal bars, those on trunk segment 14 are modified most conspicuously as large, fleshy flaps.

In *Micropacter yagerae*, all sternal bars are almost completely reduced, except on trunk segment 14, which bears an oval-shaped flap (Koenemann et al. 2007). On all remaining (anterior) trunk segments, actual 'bars' are not detectable but have been reduced to faint sutures. We decided to delete this autapomorphic condition as a separate character state (2) in matrix B, and alternatively assigned state 1 to Micropacteridae. In this case, we regarded heteromorphy as a shared derived condition for all taxa with modified bars on trunk segment 14.

5. Trunk segments
   0: 16 segments
   1: 21–22 segments
   2: 24–25 segments
   3: 27 segments
   4: 29–30 segments
   5: 32 segments
   6: 38 segments
   7: 40–41 segments
   MATRIX B: 8: 16 segments, fused

The number of trunk segments in nectiopod remipedes is probably subjected to some type of allometric growth. What appear to be juveniles and small adults seem to have fewer trunk segments than large adults. Our recent study of 139 specimens of Nectiopoda could not confidently confirm an upper limit of body size and/or segment numbers in any species investigated (Koenemann et al. 2006). The results of this study suggest that many species of remipedes do not terminate growth at a particular stage, both in regard to absolute body size and to the number of trunk segments, once they reach the reproductive adult stage. Nevertheless, we decided to include this character despite its problematic aspects. We assumed that the vast majority of all specimens we investigated do contain representative adult specimens and used the recorded maximum number of segments for each taxon.

To date, there are two species that exhibit the minimum number of recorded trunk segments, *Godzilliognomus frondosus* and *Micropacter yagerae*. We assigned state 0 to both species in matrix A. However, the trunk terminus of *Micropacter* is oval-shaped, and the segments posterior to trunk segment 14 show an advanced state of fusion, which includes the anal somite (Koenemann et al. 2007). We scored this autapomorphic modification as a separate eighth state in matrix B.

6. Antennule, segmentation of dorsal flagellum
   0: > 20 segments
   1: 18 segments
   2: 16 segments
   3: 14 segments
   4: 13 segments
   5: 12 segments
   6: 11 segments
   7: 10 segments

For characters 6 and 7, we scored the known maximum number of segments for both flagella of the antennule (see Fig. 1A, C). Although the intraspecific number of antennular segments is relatively stable in nectiopod remipedes and most other crustaceans, we did not order these two characters for two reasons. First, marked interspecific variation of segment numbers in closely related groups is not unusual. Consequently, segment numbers are probably not completely reliable semaphoronts when sampling of representative taxa is incomplete. Second, we cannot rule out evolutionary 'quantum' leaps in closely related species. In these cases, state transitions could involve several antennal segments. Therefore, ordering this character involves more (speculative) assumptions than allowing all possible state changes.

7. Antennule, ventral flagellum
   0: > 20 segments
   1: 18 segments
   2: 15 segments
   3: ca. 14 segments
   4: 12 segments
   5: 10 segments
   6: 8 segments
   7: 7 segments
   MATRIX B: 8: 3 segments
   9: ca. 2–3 segments

Both in *Godzilliognomus* and *Godzillius* (state 9) and in the speleonectid *S. benjamini* (state 3), several proximal segments of the ventral flagella are described as being fused. In these cases, it was not possible to determine a definite number of segments, and we estimated the maximum number based on the descriptions. Therefore, character states 3 and 9 are approximations of segment numbers and do not define the fusion of segments per se.

Micropacter has a very short ventral flagellum that is similar in length to the reduced flagella in *Godzilliognomus* and *Godzillius*, and we applied state 9 to *Micropacter* in analysis A. However, unlike the flagella in the two godzilliids, the short ventral flagellum in *Micropacter* is composed of three well-separated articles, without any trace of fusion, which seemed to justify the assignment of an autapomorphic character state in matrix B (state 8).

8. Maxillule, endite of third segment
   0: endite absent
   1: distinct endite with spines and/or setae
   2: endite and armature greatly reduced
   3: endite reduced, segment elongated

The absence of a third maxillulary endite in *Tesnusocaris* is considered plesiomorphic (state 0; Fig. 2B). The vast majority of nectiopod remipedes have well-developed third endites with two prominent spines and numerous setae (state 1; Fig. 2A). In *Micropacter*, *Godzilliognomus* and *Godzillius*, the third maxillulary endite is greatly reduced (state 2; Fig. 2C). The maxillule of *Pleomothra* differs considerably from those of all other remipedes in several ways (state 3). Most importantly, it is composed of six segments instead of seven (Fig. 2D). However, to be able to score characters

defining the maxillule we need to identify maxillulary segments that are homologous between *Pleomothra* and the remaining remipedes. In other words, we need to decide which limb segment is lost in *Pleomothra*.

The most straightforward way to resolve this dilemma is to first identify the main point of flexure, the elbow, in *Pleomothra*. In all Remipedia, the maxillulary elbow is located between segments four and five (Fig. 2A–C). However, in *Pleomothra* there appear to be two joints, the first situated between segments three and four, and the second between segments four and five. We assume that the first or most proximal of these points of flexure represents the original elbow, and that the other is secondarily derived. Consequently, we can exclude a loss of the fourth and fifth segments in *Pleomothra*, for several reasons.

(1) Segments four and five are part and counterpart of the elbow in all remipedes. These segments are complex functional units for the handling of food or prey. Therefore, a reduction of these segments is less likely than the loss of a segment that has a minor functional (and structural) significance, for example segments three and six.
(2) The fourth and fifth segments are also relatively long and wide maxillulary segments in all nectiopods. We argue that loss is much more probable for a segment that already exhibits a distinct reduction among taxa, e.g. for segment six, than for a well-developed segment.
(3) The fourth segment (lacertus) in *Godzillius* and *Pleomothra* is distinctly enlarged and modified. In both taxa, segment 4 lacks spines but is equipped with similar, papillary-like structures. Therefore, we assume that the fourth maxillulary segments in *Pleomothra* and *Godzillius* are homologous.

Furthermore, the unique morphology of the distal-most segment, the claw, as well as the first two proximal, endite-bearing segments suggests homology of these articles in all nectiopods (including *Pleomothra*). Thus, the lost segment in *Pleomothra* is either the third segment or segment six.

The third maxillulary segment shows similar modifications in *Godzilliognomus* and *Godzillius*. While the distal endite and its armature appear greatly reduced, this entire segment has become more robust and longer in both taxa (compared to Speleonectidae). We conclude that the elongated third segment in *Pleomothra* is not lost, but rather is a modification of the original third maxillulary segment.

The sixth maxillulary segment is characterized by varying degrees of reduction in all nectiopods. It is typically shorter than the adjacent segments five and seven, particularly in *Godzillius* (Fig. 2C). Therefore, segment six is the most likely candidate for a lost (or modified) segment in *Pleomothra*. By extension, the posterior elbow between segments four and five in *Pleomothra* is homologous to the original, main point of flexure, whereas the more anterior joint is secondarily derived (Fig. 2D).

Altogether, these morphological particulars are fragments of a mosaic outlining the evolution of remipede maxillules. The maxillule of *Godzillius* shows some unusual modifications that are similar to those observed in *Pleomothra*. In *Godzillius*, the maxillule is a remarkably large, robust appendage bearing a long medial process equipped with papillae on segment four (lacertus). Papillae are also found on the distal process of segment four in *Pleomothra*, which has by far the largest maxillule of all remipedes. The long medial process in *Godzillius* seems to represent an advanced stage in a trend towards developing a counterpart to the distal, piercing claw of a prehensile appendage. The tendency to develop such a structure, albeit less pronounced, can be observed in several other taxa, e.g. in *S. gironensis*, *S. tulumensis* and *S. lucayensis*. For this reason, *Pleomothra* may very well stand at one end of a transformation series that begins with a simple, prehensile limb (*Tesnusocaris*) evolving into a more advanced grasping-and-piercing tool and, finally, into a pseudochelate appendage (*Pleomothra*). It is possible that the peculiar subdistal process at the medial base of the claw in *Pleomothra* is a vestige of segment six.

9. Maxillule, corner spines of lacertus
   0: absent
   1: 1 or 2 slender spines
   2: 2 stout spines
   3: group of spines
   4: 1 conical spine
   5: reduced

Similar to the variable forms of enditic expansions, the medial spines of maxillulary lacerti show a remarkable degree of variation. It seems impossible to make a priori assumptions about which condition represents the nectiopod ground pattern. In the majority of species, however, we can observe one or two spines on the proximomedial margin, followed by a row of more or less slender setae. The fact that these spines occur in all instances on the apex of an enditic process or corner suggests a functional homology (see previous character). In *Godzillius* and *Pleomothra*, the maxillules are distinctly modified and lack spines on their lacerti (state 5).

10. Maxillule, size compared to maxilla
   0: maxillule smaller
   1: about subequal
   2: maxillule huge, massive

For each taxon, we compared the width and length of the maxillule to those of the adjacent posterior cephalic

limb, the maxilla. Both size categories appeared to represent discrete rather than continuous states (see Fig. 2). We also assumed that these two size dimensions of a limb may be treated as dependent variables. Therefore, we combined three discrete states of width and length comparisons in one character. The enormous maxillules of *Pleomothra* (state 2) show several peculiar modifications (Fig. 2D). Because state 2 unmistakably differs from the conditions found in other remipedes, it was applied as an autapomorphy.

11. Maxilla, segmentation of brachium
    0 (both matrices): 5 segments
    1 (both matrices): 4 segments
    2 (MATRIX A): 3 segments
    2 (MATRIX B): 3 segments, central suture
    3 (MATRIX B): 3 segments, distal suture

Another feature observable in both maxilla and maxilliped is the fusion of segments of the brachium. The five-segmented brachium (including the claw) in *Tesnusocaris* is possibly the ancestral condition for Remipedia (Fig. 2B). Hence, by accepting the main point of flexure in the prehensile limbs as homologous (see discussion of character 8) we recognize a one-step reduction to a four-segmented brachium as a synapomorphy for Nectiopoda (state 1). The Godzilliidae and Micropacteridae exhibit an even more advanced state of fusion. Their brachia are composed of three segments (state 2 in matrix A). However, in contrast to the godzilliids which have extremely slender brachia with faint distal sutures, the robust brachium in *Micropacter* is fused into two equally long segments (followed by the claw), with a distinct central suture. We cannot exclude that this condition is not homologous to the thin brachia and distal sutures in the godzilliids and defined two separate states 2 and 3 in matrix B for the three godzilliids and *Micropacter*, respectively.

12. Maxilliped, segmentation of brachium
    0 (both matrices): 5 segments
    1 (both matrices): 4 segments
    2 (MATRIX A): 3 segments
    2 (MATRIX B): 3 segments, central suture
    3 (MATRIX B): 3 segments, distal suture
    Constrained analysis: irreversible (up)

We chose to code the number of brachia segments on maxilla and maxilliped as two individual characters, because the brachia of *Godzillius* exhibit an asymmetrical reduction: the maxilliped is composed of four segments, while the maxilla has only three segments. Moreover, we believe the reductions of maxillipedal and maxillary segments are significant evolutionary modifications that justify extra weight.

Unlike the segmentation of the maxilla (character 11), the maxillipedal brachium featured two-step transitions and reversals in the unconstrained analysis of both matrices A and B (see Figs. 4 and 6). Therefore, we favored a directed, irreversible evolution of this character in the constrained runs of matrices A and B.

See comments on previous character for a justification of applying two alternative sets of character states in matrices A and B.

13. Maxillule, armature of lacertus
    0: absent
    1: few setae
    2: sparse row
    3: dense row
    4: few setae and spine row

This character quantifies the setae on the inner margin of the maxillulary lacertus. Based on the discussion of character 8, we consider the long medial process in *Godzillius* homologous to the distal process of maxillulary segment 4 in *Pleomothra*. Both processes are sparsely equipped with setae (state 1). Some taxa bear rows of setae or spines covering the inner margins of these limbs almost continuously (state 3; Fig. 2C, D). In contrast to this presumably advanced state is a distinguishable degree of less dense covering (state 2; Fig. 2A).

Characters 13–15 do not distinguish between different setal types. They describe the density of setae and spines on the inner margins of maxillary and maxillipedal lacerti and brachia. We treated the modification of spines/setae in characters 16 and 17.

14. Maxilla and maxilliped, armature of lacertus
    0: covering 30–50% of margin
    1: dense, covering ca. 75% of margin
    2: dense, on entire margin

In all remipedes, both maxilla and maxilliped are prehensile appendages with a high degree of structural similarity, and are morphologically very distinct from the prehensile maxillule. Similar to the armature on the maxillulary lacertus (previous character), the inner margins of maxillary and maxillipedal lacerti can be almost continuously covered (state 2; Fig. 2C, D). In contrast to this presumably advanced state are two distinguishable degrees of less dense covering (states 0 and 1; Fig. 2A, B).

Because the setal cover on lacerti and brachia varied among taxa, we treated the armature on these segmental units as two separate characters.

15. Maxilla and maxilliped, armature of brachium
    0: sparse, covering less than 50% of margin
    1: sparse, covering more than 75% of margin
    2: dense, covering ca. 75% of margin
    3: dense, on entire margin

16. Maxilla and maxilliped, setal pattern of lacertus and brachium
    0: isomorphic
    1: heteromorphic

Maxillary and maxillipedal setae (or spines) can be different on lacerti and brachia, respectively. This character distinguishes between similar (isomorphic) and unequal (heteromorphic) types of setae/spines on lacertus and brachium. For example, in the three godzilliids the setae/spines on the lacerti are much longer and more robust than those on the brachia (Fig. 2C, D). By contrast, Speleonectidae and Micropacteridae have isomorphic setae/spines on their lacerti and brachia.

17. Maxilla and maxilliped, setal types of lacertus
    0: simple setae
    1: plumose setae
    2: candeliform setae
    3: discoid organs

This character describes several types of setal modifications. States 2 and 3 are autapomorphies both for *Pleomothra* and *Cryptocorynetes*. The maxillae and maxillipeds in *Cryptocorynetes* bear discoid organs that may facilitate holding on to active prey this remipede may have specialized to feed upon. Since the discoid organs of *Cryptocorynetes* are an autapomorphy, with no transitional forms known, we can only speculate whether they are derived from setae or spines, or a different type of cuticular outgrowth. However, it is worth to point out that the papillae on the maxillules of *Godzillius* and *Pleomothra* bear a certain resemblance to the discoid organs of *Cryptocorynetes*. There may be a shared morphogenetic mechanism that controls this type of modification in remipedes. We believe that this character deserves more detailed attention in future analysis, since setal patterns may contain a significant phylogenetic signal.

18. Maxilla and maxilliped, length ratio of brachia
    0: subequal
    1: maxilliped longer

In most speleonectid taxa, the brachium of the maxilliped is distinctly longer than that of the maxilla (state 1). In *Micropacter* and the three godzilliids, however, both brachia are approximately equal in length (state 0).

19. Sectorization of maxilla
    0: absent
    1: weak
    2: well-developed
    3: distinct

The structural division at the elbow in maxillae and maxillipeds can be more or less developed. Some taxa have particularly narrow brachia, while the lacertus tends to become wider and longer (Fig. 2). This sectorization of both appendages is most noticeably developed in the godzilliids (state 3; Fig. 2C, D). While a structural subdivision of the maxilla is lacking in *Tesnusocaris* (state 0), the speleonectids exhibit varying degrees of sectorization (states 1 and 2; Fig. 2A). Because in some taxa the sectoring of the maxilla is more strongly developed than that of the maxilliped, we assigned separate characters for both limbs (following character).

20. Sectorization of maxilliped
    0: absent
    1: weak
    2: well-developed
    3: distinct

See previous character for detailed comments.

21. Terminal claw of maxilla
    0: simple nail
    1: longfinger-type
    2 *Godzillius*-type
    3: horseshoe with 7–10 denticles
    4: horseshoe with 13 denticles
    5: horseshoe with 17–20 denticles
    6: horseshoe with ca. 30 denticles
    Constrained analysis: step matrix

We consider the unique variation of maxillary and maxillipedal claw types as one of the key characters towards understanding the evolution of Remipedia. In Nectiopoda, these claws are complex and represent a deviation from the simple claw found in *Tesnusocaris* (state 0; Fig. 2B). Indeed, the claws of maxillae and maxillipeds of nectiopods are distinct autapomorphies within the Crustacea. We recognize four types of claws (Fig. 3). The 'longfinger-type', with one prominent, long spike accompanied by several small, pointed denticles may represent a plesiomorphic condition (state 1; Fig. 3D). The claws of godzilliids have a grappling-hook appearance, with several sharply pointed, long denticles (state 2; Fig. 3C). The four 'horseshoe-types' can be distinguished by the number of denticles arranged in a semi-circular array. For example, the claws of *S. parabenjamini* are composed of 7–8 somewhat incised denticles (state 3; Fig. 3A). In *S. tanumekes*, the distal margin of the horseshoe bears a fine, even serration, with about 20 small denticles (state 5; Fig. 3B).

The single known species of Micropacteridae is the only remipede with unequal claw types on maxilla and maxilliped. Therefore, we devised separate characters for maxillary and maxillipedal claws, respectively. This separation concerns characters 21–24 (see Koenemann et al. 2007 for a description of the claws in *Micropacter*).

In the unconstrained analyses of matrices A and B, the fused horseshoe-type of claw (state 3) is reversed into claw types with more or less free denticles (states 1 and 2; see Figs. 4 and 6). We considered this transition unlikely and designed a step matrix to constrain state transitions for this character (Table 1).

22. Terminal claw of maxilliped
    0: simple nail
    1: longfinger-type
    2 Godzillius-type
    3: horseshoe with 7–10 denticles
    4: horseshoe with 13 denticles
    5: horseshoe with 17–20 denticles
    6: horseshoe with 30 denticles
    Constrained analysis: step matrix

In the constrained analyses, the step matrix shown in Table 1 was used to rule out improbable character reversals (see previous character).

23. Maxilla, length of dominant denticle of claw
    0: simple nail
    1: dominant denticle much longer and stouter than satellite denticles
    2: dominant denticle somewhat longer than satellite denticles
    3: all denticles equally long
    4: dominant denticle reduced, small

Characters 21 and 22 deal with the varying number of denticles that form the claws of maxillae and maxillipeds. The second-from-lateral denticle is typically longer and stouter than the remaining, smaller satellite denticles (Fig. 3). We compared the length of the most prominent (central) denticle to that of the smaller associated ones. A reduced denticle (state 4) was observed only in horseshoe-types of claws.

Table 1. Step matrix for character states 0–6; x = forbidden reversal

	0	1	2	3	4	5	6
0	—	1	2	2	2	2	2
1	*x*	—	1	2	2	2	2
2	*x*	*x*	—	1	1	1	1
3	*x*	*x*	*x*	—	1	1	1
4	*x*	*x*	*x*	*x*	—	1	1
5	*x*	*x*	*x*	*x*	*x*	—	1
6	*x*	*x*	*x*	*x*	*x*	*x*	—

The likelihood of transitions is defined by the number of steps needed to advance from one state to another. For example, the longfinger-type of claw (state 1) seems morphologically closest to the plesiomorphic simple nail in *Tesnusocaris* (state 0). However, further assumptions regarding state transitions are speculative. Therefore, all remaining claw types (states 2–6) are scored as equally distant from state 1. Moreover, we believe that each individual nectiopod claw type (states 1–6) represents a unique specialization, and thus we excluded the possibility of reversals among these states.

24. Maxilliped, length of dominant denticle of claw
    0: simple nail
    1: dominant denticle much longer and stouter than satellite denticles
    2: dominant denticle somewhat longer than satellite denticles
    3: all denticles equally long
    4: dominant denticle reduced, small

25. Length of caudal rami
    0: long cerci
    1: 2–2.5 times anal somite
    2: ca. 1.5 times anal somite
    3: slightly longer than anal somite
    4: as long as or shorter than anal somite
    5: rudimentary

The length of the caudal rami was compared to the length of the anal somite (Fig. 1A, C). State 3 represents caudal rami that were slightly longer than the anal somite. State 4 was applied to caudal rami that were slightly shorter than or as long as the anal somite.

26. Anal somite, relation of length to width
    0: wider than long
    1: as long as wide
    2: longer than wide
    3: fused to trunk

This character describes the width/length proportions of the anal somite.

Results

We applied two sets of coding options (unconstrained versus constrained) to two alternative matrices (Figs. 4–8). This combined approach resulted in four different trees. In addition, we conducted analyses with reweighted characters, bootstrap analyses, and an analysis from which the new family Micropacteridae was excluded. Some of the trees resulting from the analyses had identical or compatible branching patterns. Therefore, only trees with conflicting topologies are presented as figures herein; less well-resolved trees that are compatible with one of the trees shown in Figs. 4–8 are not shown but described below. An overview of methodological combinations and resulting trees is given in Table 2.

Matrix A (Figs. 4 and 5)

The unconstrained parsimony analysis of 26 unordered (and unweighted) characters yielded 86 maximum

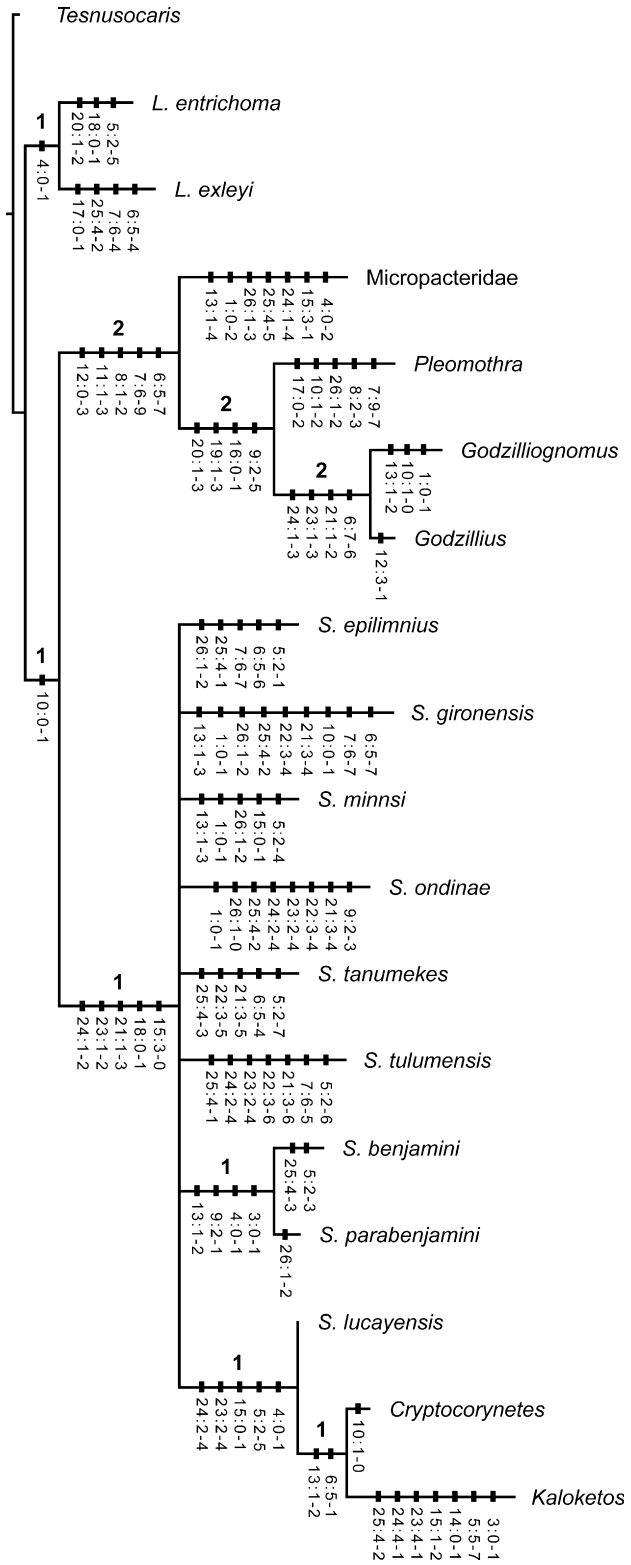

Fig. 4. Matrix A: unconstrained parsimony analysis (all characters unordered). Strict consensus tree of 86 trees found (length = 146; min/max lengths = 92/209; CI = 0.630; RI = 0.538; RC = 0.339; HI = 0.370). Large numbers on internal branches represent decay indices. Small numbers show unambiguous state changes (occurring in all possible reconstructions) for terminal taxa and internal nodes (see also text in "Characters and character states").

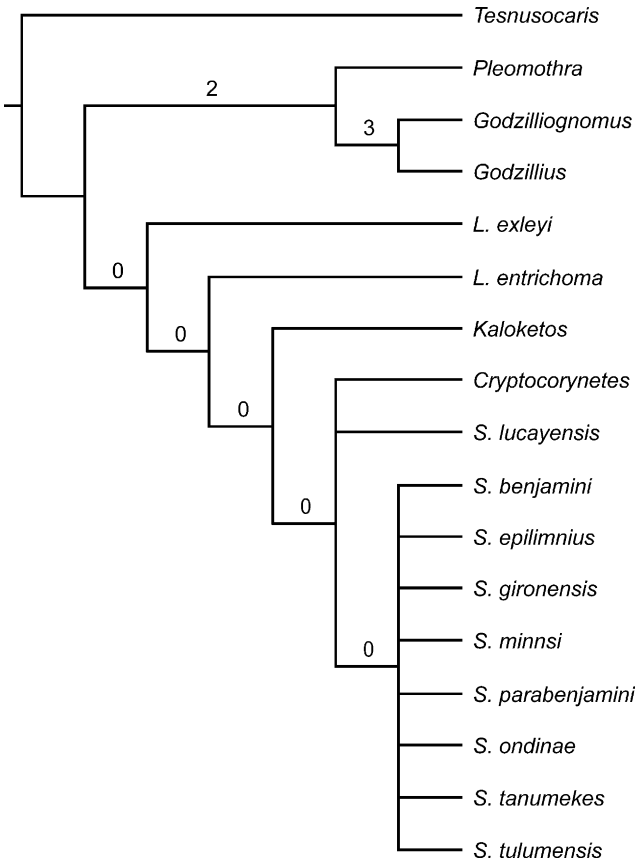

Fig. 5. Matrix A: unconstrained parsimony analysis (all characters unordered), Micropacteridae excluded. Strict consensus tree of 39 trees found (length = 138; min/max lengths = 86/192; CI = 0.623; RI = 0.509; RC = 0.317; HI = 0.377). Numbers on internal branches represent decay indices.

parsimonious trees (MPT). In the strict consensus tree, the family Speleonectidae emerges as a paraphyletic group (Fig. 4). The two species of the speleonectid genus *Lasionectes* form a sister group to two larger clades: the Godzilliidae with the new family Micropacteridae as a basal sister group, and the remaining three genera of the family Speleonectidae on a clade with poor resolution. The decay indices for individual clades are not higher than 2.

A second analysis of the unconstrained data set, this time excluding Micropacteridae, resulted in 39 trees. The Speleonectidae are now monophyletic, with two species of *Lasionectes* as basal paraphyletic sister taxa (Fig. 5). However, the decay indices for the Speleonectidae and clades within this group are zero, which means that these topologies were not present in all, but only in some of the 39 resulting trees.

Although in the constrained analysis only 33 MPTs were found, the resolution of the strict consensus tree is even lower than in the unconstrained analysis (length = 160; min/max lengths = 87/240; CI = 0.544;

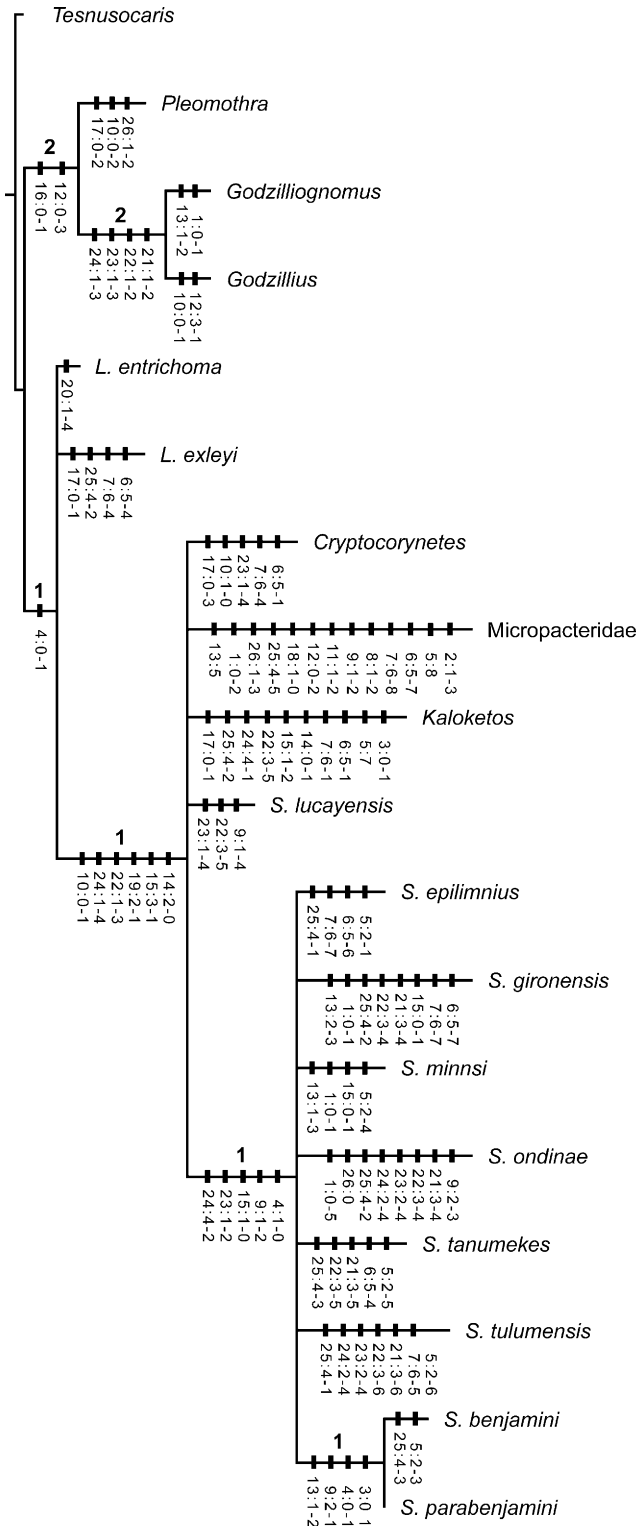

Fig. 6. Matrix B: unconstrained parsimony analysis (all characters unordered). Strict consensus tree of 48 trees found (length = 152; min/max lengths = 95/209; CI = 0.625; RI = 0.500; RC = 0.312; HI = 0.375). Large numbers on internal branches represent decay indices. Small numbers show unambiguous state changes (occurring in all possible reconstructions) for terminal taxa and internal nodes (see also text in "Characters and character states").

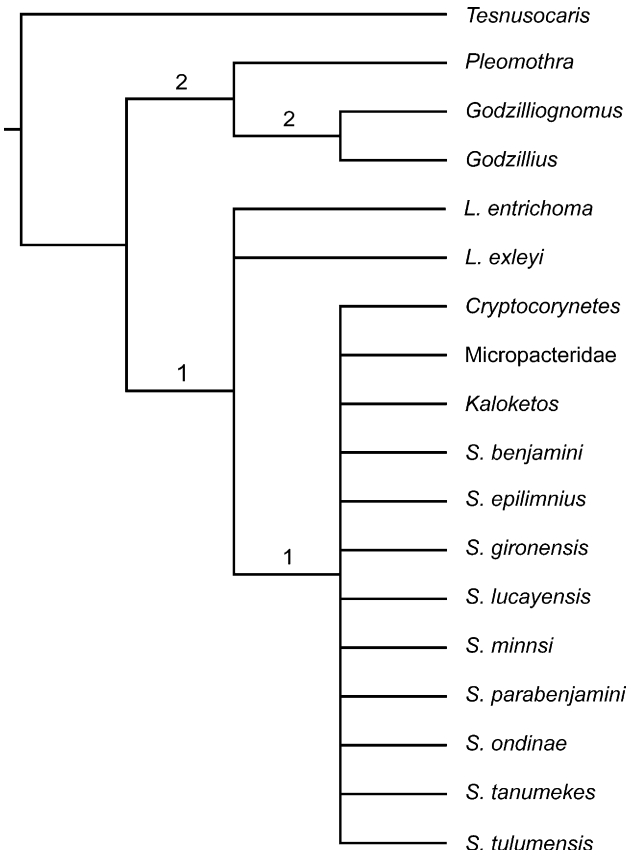

Fig. 7. Matrix B: constrained parsimony analysis (some characters irreversible or otherwise constrained). Strict consensus tree of 174 trees found (length = 170; min/max lengths = 89/239; CI = 0.524; RI = 0.460; RC = 0.241; HI = 0.476). Numbers on internal branches represent decay indices.

RI = 0.523; RC = 0.284; HI = 0.456). Since the main branching pattern of this cladogram is identical with that of the unconstrained analysis, we do not show the constrained tree here. The only deviation from the unconstrained topology is that the two clades with [*Speleonectes benjamini* + *S. parabenjamini*] and [*S. lucayensis*, [*Cryptocorynetes* + *Kaloketos*]] have collapsed and form a polytomous array with most of the remaining species of *Speleonectes*, and that a new dichotomy with [*S. gironensis* + *S. minnsi*] has emerged instead. Similar to the unconstrained analysis, all clades are weakly supported by decay indices between 1 and 2.

The reweighted analysis of the unconstrained data set resulted in 33 MPTs, of which a strict consensus tree was calculated (Fig. 8). The Speleonectidae now emerge as a monophyletic group on a mostly resolved clade with a paraphyletic internal branching pattern. In the reweighted analysis of the constrained matrix (not shown), only the clade with Micropacteridae and the three godzilliids is sustained. All other taxa, including the two species of *Lasionectes* and the outgroup *Tesnusocaris*, appear as polytomous terminal taxa.

Similarly, a bootstrap analysis (not shown) of the unconstrained matrix yielded a mostly polytomous clade with all Nectiopoda. There were only two resolved clades: [Micropacteridae, [*Pleomothra*, [*Godzillius* + *Godzilliognomus*]]] with a bootstrap support of 68%, and [*S. benjamini* + *S. parabenjamini*] with 51% support. The highest bootstrap support was found for the clade with *Godzillius* and *Godzilliognomus* (88%).

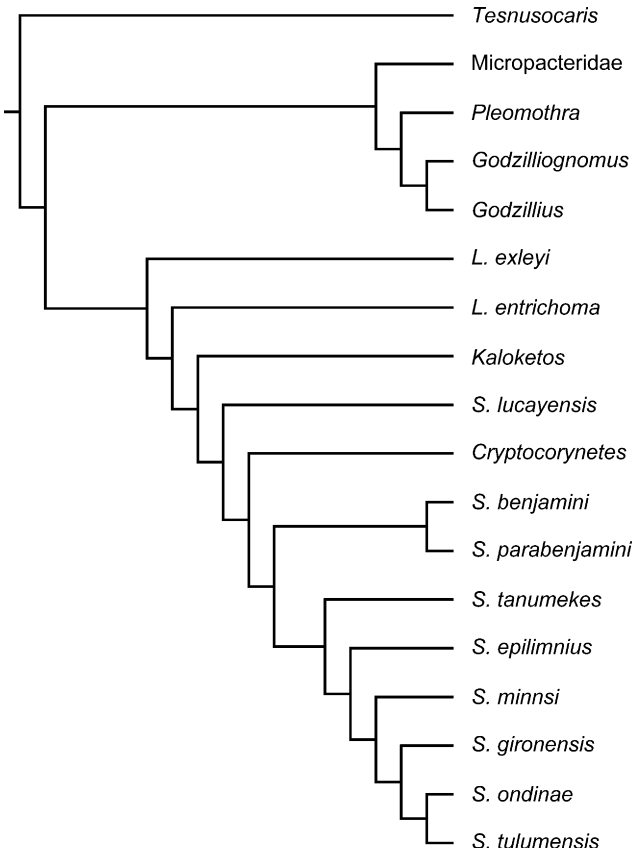

Fig. 8. Matrix A: reweighted unconstrained parsimony analysis (all characters unordered but reweighted, see text in "Reweighting characters"). Strict consensus of 33 MPTs (length = 60.23005; min/max lengths = 44.77453/101.84005; CI = 0.743; RI = 0.729; RC = 0.542; HI = 0.257).

Matrix B (Figs. 6 and 7)

The unconstrained analysis of matrix B resulted in 48 trees. Although the general topology of the strict consensus tree compares well with the results obtained from analyses of matrix A, there are some significant inconsistencies (Fig. 6). The most decisive difference concerns the position of the Micropacteridae, which now appears within a large clade composed of all taxa currently assigned to the Speleonectidae. The Speleonectidae and Godzilliidae are sister groups. The speleonectid clade features the two species of *Lasionectes* as basal paraphyletic branches, followed by a polytomous array comprising *Cryptocorynetes*, *Kaloketos*, Micropacteridae, *S. lucayensis*, and a poorly resolved clade with the remaining eight species of *Speleonectes*.

The strict consensus tree obtained by the constrained analysis of matrix B is similar to the unconstrained tree, although the clade with eight species of *Speleonectes* has collapsed. The new family Micropacteridae appears on a large polytomous clade together with *Cryptocorynetes*, *Kaloketos*, and all species of *Speleonectes* (Fig. 7).

The support for individual clades in both constrained and unconstrained analyses is again weak, with decay indices between 1 and 2.

In the reweighted analyses of the unconstrained analyses, almost all taxa that appeared as polytomous branches (in the unweighted run) are now arranged in a paraphyletic branching pattern (Fig. 9). By contrast, the reweighted analysis of the constrained data set produced an almost completely unresolved consensus tree (not shown). Only one clade containing the three godzilliids is sustained. Similar to the reweighted constrained run of matrix A, all other taxa appear as polytomous terminal taxa.

The bootstrap analysis of the unconstrained analysis produced a tree that is almost identical with the bootstrap tree obtained from matrix A (not shown). The only difference is that *Micropacter* no longer clusters with the three godzilliids, but joins a large polytomy together with 12 speleonectids. The two

Table 2. Overview of trees resulting from analytical and methodological alternatives used in this study

	Matrix A		Matrix B	
	Unconstrained run	Constrained run	Unconstrained run	Constrained run
Parsimony analysis	Strict consensus of 86 trees (Fig. 4)	Strict consensus of 33 trees (not shown)	Strict consensus of 48 trees (Fig. 6)	Strict consensus of 174 trees (Fig. 7)
Reweighted analysis	Strict consensus of 33 trees (Fig. 8)	Strict consensus of 405 trees (not shown)	Strict consensus of 9 trees (Fig. 9)	Strict consensus of 261 trees (not shown)
Micropacteridae excluded	Strict consensus of 39 trees (Fig. 5)			
Bootstrap analysis	1 tree (not shown)		1 tree (not shown)	

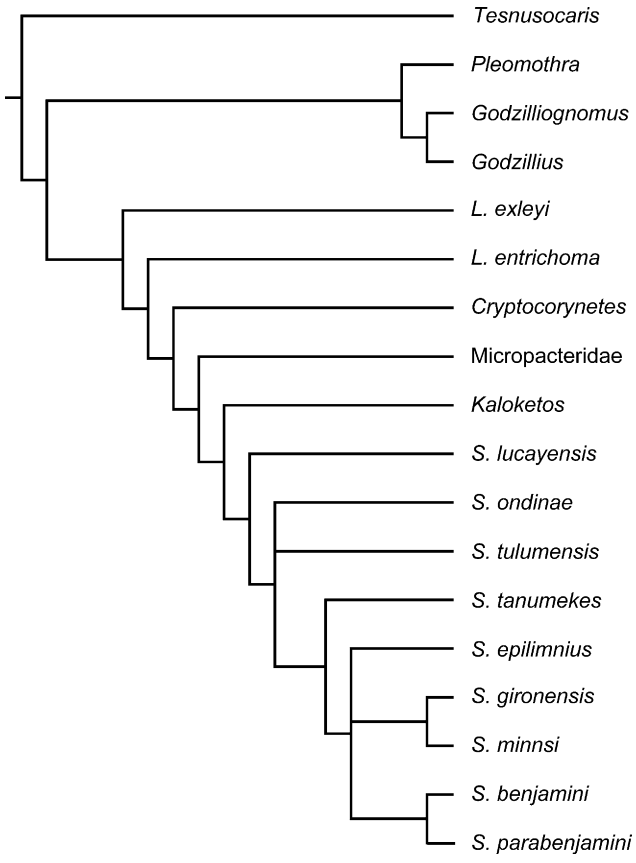

Fig. 9. Matrix B: reweighted unconstrained parsimony analysis (all characters unordered but reweighted, see text in "Reweighting characters"). Strict consensus tree of 9 trees found (length = 62.56104; min/max lengths = 48.83414/110.81112; CI = 0.781; RI = 0.779; RC = 0.608; HI = 0.219).

resolved clades contain again the three species of the family Godzilliidae [*Pleomothra*, [*Godzillius* + *Godzilliognomus*]], bootstrap values = 91% and 94%, respectively, and (again) a dichotomous clade with *S. benjamini* and *S. parabenjamini* (bootstrap value = 52%).

Discussion

Comparative morphology of maxillule, maxilla and maxilliped

The three prehensile cephalic limbs, maxillule, maxilla and maxilliped, embody important diagnostic characters of remipede crustaceans. Taken as a morphological and functional unit, the grasping and piercing apparatus composed of these three appendages is distinctive for each species of remipede. Each individual set of limbs is distinguished by a unique combination of characters, so that there are no two sets of prehensile limbs absolutely alike among all remipede species. By this, the raptorial limbs stand out from probably all other diagnostic characters, e.g. antennules, antennae, paddle-shaped trunk limbs, etc., all of which show little morphological variability. Therefore, the cephalic limbs serve as excellent 'fingerprints' or markers to identify and determine remipedes. However, this high degree of differentiation at first glance complicates phylogenetic analyses. If everything is unique, how does one deduce relationships? It is only by breaking down these complex limbs into their structural components that similarities and differences emerge. When this is done, these limbs can provide critical clues regarding the evolution of remipedes, as well as the cephalic–thoracic tagmata boundary in crustaceans.

There are several intriguing questions concerning the prehensile limbs of Remipedia. What is the plesiomorphic condition regarding the number of segments in these appendages? Did all three limbs have the same or different numbers of segments in ancestral remipedes? How do the post-oral limbs in remipedes accord with *Hox* gene expression patterns known from other arthropods?

To answer these questions, we would first need to be able to assess homologies of individual segments in the two remipede orders Enantiopoda and Nectiopoda. The Enantiopoda contain two extinct taxa, *Tesnusocaris goldichi* (our outgroup) and the Carboniferous fossil *Cryptocaris hootchii*. Unfortunately, the segmentation of the three prehensile cephalic appendages in *Cryptocaris* is not completely known (Emerson and Schram 1991). Therefore, *Tesnusocaris* is the only available outgroup taxon for a comparison with the order Nectiopoda, which exclusively embrace all living remipedes.

Contrary to the condition in the maxillule and maxilla, the proximal-most segments of the maxilliped in nectiopods lack endites and the basal-most segments are comparably short. For these reasons, the unambiguous identity of individual segments remains difficult to determine in some taxa. The maxillipeds of a number of remipedes are described as being composed of eight segments. However, a re-examination of reserve collection and type material did not confirm this. Maxillipeds appear to be nine-segmented in all specimens we examined (although some taxa in the Speleonectidae and Godzilliidae show a tendency to reduce both size and degree of articulation of the basal segments). For example, in the original description of *S. tulumensis* from the Yucatan Peninsula, the maxilliped was said to have eight segments (Yager 1987b), whereas a later study confirmed a nine-segmented maxilliped for *S. tulumensis* (Felgenhauer et al. 1992).

The number 9 attains some added interest when these limbs are compared to what Emerson and Schram (1991) referred to as the endopeds [sic] of the trunk limbs of *Tesnusocaris*. These limbs also consist of nine segments. One can also find limbs consisting of large

numbers of segments in many Cambrian arthropods, such as *Ercaia minuscula* (Chen et al. 2001), *Canadaspis laevigata* (Hou and Bergstrom 1991), *Retifacies abnormalis* (Hou et al., 1989) and *Fuxianhuia protensa* (Hou 1987). What the significance of this may be deserves a more detailed consideration elsewhere. Obviously, we can at least say that there is a tendency towards reduction and fusion in each of the three limbs in nectiopods.

While the maxillipeds of the fossil *Tesnusocaris* have well-separated, simple, basal segments, the basalmost three segments in nectiopods form a sequence of articles with joints perpendicular to the limb axis. They are interlocked, with complex, oblique articulations (Fig. 2). It is possible that this complex arrangement functions as a sort of universal joint allowing vertical and horizontal movement of the maxillipeds.

Taxonomy of Remipedia

The taxonomy of any newly recognized group is of necessity merely a cataloging system – names loosely grouped to impose some rudimentary order on the biodiversity. However, once sufficient numbers of species become known in more detail, cladistic analyses of relationships can be performed. At that point, a more natural system of classification can emerge, one that more adequately reflects the nested sets of apomorphies that define groups than the first-order cataloging taxonomy.

We decided not to present here a revision of the remipede system of classification. We think additional data are needed to substantiate such a revision. Taxonomies, like cladograms themselves, are approaches towards complex (phylogenetic) relationships. These hypotheses need to be tested against new knowledge and fresh insights, and may eventually contribute to deeper understanding of a group's biodiversity. Through this, they serve as road maps to guide future research.

The family Godzilliidae, with the three monotypic genera *Godzillius*, *Godzilliognomus* and *Pleomothra*, is the only taxon that emerged as a trichotomous clade in all analyses. In all instances, *Pleomothra* was the sister group to [*Godzillius* + *Godzilliognomus*]. At this point, we accept this stable pattern as support for a monophyletic Godzilliidae. However, the only apomorphies that *Pleomothra* shares with *Godzillius* and *Godzilliognomus* are the sectorized and fused brachia of maxilla and maxilliped. *Pleomothra* does not share any of the additional advanced modifications that serve to diagnose the Godzilliidae, for example a very short, fused ventral antennular ramus, a reduced third maxillular endite, and the grappling-hook type of claws on maxilla and maxilliped. Therefore, a separate familial status for *Pleomothra* may be indicated. However, we think that the results presented herein do not support higher-level revision at this point. We are currently investigating DNA sequence data of nine genes, in addition to the morphological characters, to evaluate phylogenetic relationships within the Nectiopoda more accurately.

There is uncertainty about the status of the genus *Lasionectes*; it is a paraphyletic genus in the analysis of matrix A, as part of a basal sister clade to a clade with the Godzilliidae + Micropacteridae, and a large, poorly resolved clade composed of the remaining speleonectid taxa (Fig. 4). However, another branch-and-bound search of matrix A, this time with Micropacteridae excluded from the analysis, succeeded in maintaining monophyly of the Speleonectidae (Fig. 5). This result is comparable with the phylogeny obtained from analysis B. In all instances of a monophyletic Speleonectidae, however, *Lasionectes* maintains a basal paraphyletic position, while the monophyly of *Speleonectes* is not supported: The genera *Kaloketos* and *Cryptocorynetes* tend to cluster with *S. lucayensis*. Our results appear to conflict with the current taxonomy within the Speleonectidae. However, more data, preferably molecular sequences, are required to corroborate this view.

The genus *Cryptocorynetes* is amongst the most distinctive of all nectiopods; its unique discoid organs on the maxillae and maxillipeds rival the equally attention-getting maxillules of *Pleomothra* and *Godzillius*. Yet in the unconstrained analysis, *Cryptocorynetes* emerges within the genus *Speleonectes*. This seems clearly nonsensical to us. The distinctive arrangement of the lacerti and brachia of the maxillae and maxillipeds, armed with conspicuous discoid organs, parallel the features that define the understanding of the family Godzilliidae, or the new family Micropacteridae. From a comparative morphological point of view, we believe that *Cryptocorynetes* should be allocated its own family.

Status of Micropacteridae

The two key objectives of our phylogenetic analysis of Remipedia were (1) to evaluate the validity of the present taxonomic structure within the class and (2) to determine the position of the new family Micropacteridae within the order Nectiopoda.

It is important to note that the new family is monotypic, i.e. represented by a single species in the matrix, and that it is morphologically distinguished by several unique autapomorphies. With regard to cladistic criteria, both properties pose a dilemma. It is per definition not possible to recognize a higher taxon represented by a single species as a monophyletic clade. We understand a monophylum as a hierarchical system of descent, including an ancestor (stem species) and all of its descendants. Thus, a monophyletic group is

composed of reproducing entities (species) that share at least one evolutionary novelty, or apomorphy. Consequently, the term monophylum cannot be applied to a single species or organism.

Moreover, in parsimony analyses, autapomorphies are uninformative. Their inclusion affects only the length of the resulting tree(s); the branching pattern of a particular search remains unchanged. Nonetheless, autapomorphies are significant characters for the hierarchical classification system.

In the analysis of Remipedia, we need to particularly consider the combination of these two issues, i.e. a monotypic family Micropacteridae set apart by several conspicuous autapomorphies. The latter include, for example, an ovate, fused body terminus; almost completely reduced sternal bars and pleurotergites; unequal claw types on maxillae and maxillipeds; and a molar process with a few strong denticles (spines). Some of these autapomorphies could not be incorporated as possible informative characters or states in multi-state characters.

The alternative interpretation of five autapomorphic character states in matrices A and B yielded two incompatible phylogenies. The most significant differences concern the positions of the Micropacteridae (represented by *Micropacter*) and the genus *Lasionectes*.

Analysis B seems to confirm the present taxonomy of the Remipedia (Figs. 6–8). The families Godzilliidae and Speleonectidae appear as monophyletic sister clades, with the new family Micropacteridae nested within the Speleonectidae. The results of analysis A, however, are not compatible with the current taxonomic classification of the order Nectiopoda. The Speleonectidae are paraphyletic and the Micropacteridae now emerge as a sister group of the Godzilliidae.

Our analysis of two matrices is based on alternative interpretations of five characters in *Micropacter* (see characters 4, 5, 7, 11, 12 under ''Characters and character states''). All five characters concern reductions or modifications in combination with reductions. The results of these analyses are ambiguous with regard to the status of Micropacteridae, i.e. there is no robust support for an assignment of *Micropacter* to either one of the two families, Godzilliidae or Speleonectidae. Therefore, we think that a separate familial status is justified.

Acknowledgments

This study was supported by a grant from the German Research Society to S. Koenemann (DFG KO 3483/1-1). Investigations of anchialine cave fauna of the Bahamas were supported by award number DEB-0315903 from the US National Science Foundation's Biodiversity Surveys and Inventories Program to Thomas Iliffe. Collection of specimens was carried out under a permit from the Bahamas Department of Fisheries.

Appendix A

Matrix A with 26 morphological characters. For alternative codings in matrix B see text in ''Characters and character states''.

Char. no.	1 1 1 1 1 1 1 1 1 1 1 2 2	2 2 2 2 2
Taxon	1 2 3 4 5 6 7 8 9 0 1 2 3 4 5 6 7 8 9 0 1	2 3 4 5 6
Tesnusocaris	? 0 0 0 ? 0 0 0 0 0 0 0 0 ? ? 0 0 0 0 0 0	0 0 0 0 0
Cryptocorynetes	0 1 0 1 5 1 4 1 1 0 1 0 2 0 1 0 3 1 1 1 3	3 4 4 4 0/1
Godzilliognomus	1 2 0 0 0 6 9 2 5 0 2 2 2 2 3 1 0 0 3 3 2	2 3 3 4 1
Godzillius	0 2 0 0 4 6 9 2 5 1 2 1 1 2 3 1 0 0 3 3 2	2 3 3 4 1
Micropacteridae	2 3 0 2 0 7 9 2 2 1 2 2 4 0 1 0 0 0 1 1 1/2	3 1 4 5 3
Kaloketos	0 1 1 1 7 1 1 1 1 1 1 0 2 1 2 0 1 1 1 1 5	5 1 1 2 1
L. entrichoma	0 1 0 1 5 5 6 1 1 0 1 0 3 2 3 0 0 1 2 2 1	1 1 1 4 1
L. exleyi	? 1 0 1 2 4 4 1 ? 0 1 0 3 2 3 0 1 0 2 1 1	1 1 1 2 1
Pleomothra	0 2 0 0 2 7 7 3 5 2 2 2 1 2 3 1 2 0 3 3 1	1 1 1 4 2
S. benjamini	0 1 1 1 3 2 3 1 1 1 1 0 2 0 0 0 0 1 1 1 3	3 2 2 3 1
S. epilimnius	0 1 0 0 1 6 7 1 2 1 1 0 1 0 0 0 0 1 1 1 3	3 2 2 1 2
S. gironensis	1 1 0 0 2 7 7 1 2 1 1 0 3 0 1 0 0 1 1 1 4	4 2 2 2 2
S. lucayensis	0 1 0 1 5 5 6 1 4 1 1 0 1 0 1 0 0 1 1 1 5	5 4 4 4 1
S. minnsi	1 1 0 0 4 5 6 1 2 1 1 0 3 0 1 0 0 1 1 1 3	3 2 2 4 2
S. parabenjamini	0 1 1 1 2 3 2 1 1 1 1 0 2 0 0 0 0 1 1 1 3	3 2 2 4 2
S. ondinae	1 1 0 0 2 5 6 1 3 1 1 0 1 0 0 0 0 1 1 1 4	4 4 4 2 0
S. tanumekes	0 1 0 0 7 4 6 1 2 1 1 0 1 0 0 0 0 1 1 1 5	5 2 2 3 1
S. tulumensis	0 1 0 0 6 5 5 1 2 1 1 0 1 0 0 0 0 1 1 1 6	6 4 4 1 1

Appendix B

Present classification of Remipedia (including undescribed species), and areas of known distribution. TL = type locality.

Godzilliidae

Godzilliognomus frondosus Yager, 1989. Bahamas – Sweetings Cay (adjacent to Grand Bahama Island): Sagittarius Cave (TL), Virgo Cave, Lucy's Cave; Grand Bahama Island: Asgard Cave; Abaco Island: Dan's Cave.

Godzilliognomus n.sp. Bahamas – Great Guana Cay (Exuma Cays): Oven Rock Cave; Cat Island: Big Fountain Blue Hole.

Godzillius robustus Schram et al., 1986. Turks and Caicos Islands – North Caicos Island: Cottage Pond (TL); Bahamas – Great Exuma Island: Basil Minns Blue Hole.

Pleomothra apletocheles Yager, 1989. Bahamas – Abaco Island: Dan's Cave (TL); Sweetings Cay: Sagittarius Cave.

Pleomothra n.sp. Bahamas – Great Guana Cay: Oven Rock Cave.

Micropacteridae

Micropacter yagerae Koenemann et al., 2007. Turks and Caicos Islands – Providenciales Island: Airport Cave (TL), Old Blue Hill Cave.

Speleonectidae

Cryptocorynetes haptodiscus Yager, 1987a. Bahamas – Abaco Island: Dan's Cave (TL); Grand Bahama Island: Old Freetown Cave System.

Cryptocorynetes n.sp. Bahamas – Great Guana Cay: Oven Rock Cave.

Kaloketos pilosus Koenemann et al., 2004. Turks and Caicos Islands – North Caicos Island: Cottage Pond.

L. entrichoma Yager & Schram, 1986. Turks and Caicos Islands – Providenciales Island: Old Blue Hill Cave (TL), Airport Cave; North Caicos Island: Cottage Pond.

Lasionectes exleyi Yager & Humphreys, 1996. Western Australia – Cape Range Peninsula: Cave C-28 (TL).

Speleonectes benjamini Yager, 1987a. Bahamas – Grand Bahama Island: Asgard Cave (TL); Sweetings Cay: Sagittarius Cave; Abaco Island: Dan's Cave.

S. epilimnius Yager & Carpenter, 1999. Bahamas – San Salvador Island: Major's Cave (TL).

S. gironensis Yager, 1994. Cuba – Matanzas Province: Cueva de los Carboneros (TL).

S. lucayensis Yager, 1981. Bahamas – Grand Bahama Island: Lucayan Cavern (TL); Cat Island: Big Fountain Blue Hole.

S. minnsi Koenemann et al., 2003. Bahamas – Great Exuma Island: Basil Minns Blue Hole (TL).

S. ondinae (Garcia-Valdecasas, 1984). Canary Islands – Lanzarote: Tunel de la Atlantida (TL).

S. parabenjamini Koenemann et al., 2003. Bahamas – Great Exuma Island: Basil Minns Blue Hole (TL).

S. tanumekes Koenemann et al., 2003. Bahamas – Great Exuma Island: Basil Minns Blue Hole (TL).

S. tulumensis Yager, 1987b. Mexico – Quintana Roo: Cenote Carwash (TL), Cenote Najaron.

Speleonectes n.sp. cf. *tulumensis*. Mexico – Quintana Roo: Cenote Crustacea.

Speleonectes n.sp. A. Bahamas – Cat Island: Gaitor's Blue Hole.

Speleonectes n.sp. B. Dominican Republic – Distrito Nacional: Cueva Taína, Cueva Los Jardines Orientales.

References

Chen, J.-Y., Vannier, J., Huang, D.-Y., 2001. The origin of crustaceans: new evidence from the Early Cambrian of China. Proc. R. Soc. London (B) 268, 2181–2187.

Emerson, M.J., Schram, F.R., 1991. Remipedia. Part 2. Paleontology. Proc. San Diego Soc. Nat. Hist. 7, 1–52.

Fanenbruck, M., Harzsch, S., Wägele, J.W., 2004. The brain of the Remipedia (Crustacea) and an alternative hypothesis on their phylogenetic relationships. PNAS 101, 3868–3873.

Felgenhauer, B.E., Abele, L.G., Felder, D.L., 1992. Remipedia. In: Harrison, F.W., Humes, A.G. (Eds.), Microscopic Anatomy of Invertebrates, Vol. 9. Crustacea. Wiley-Liss, Inc., New York.

Garcia-Valdecasas, A., 1984. Morlockiidae new family of Remipedia (Crustacea). Eos 60, 329–333.

Harzsch, S., 2004. The tritocerebrum of Euarthropoda: a "non-drosophilocentric" perspective. Evol. Dev. 6, 303–309.

Hou, X.-G., 1987. Three new large arthropods from Lower Cambrian Chengjiang, eastern Yunan. Acta Palaeont. Sin. 26, 273–285.

Hou, X.-G., Bergstrom, J., 1991. The arthropods of the Lower Cambrian Chiangjiang fauna with relationships and evolutionary significance. In: Simonetta, A.M., Conway Morris, S. (Eds.), The Early Evolution of Metazoa and the Significance of Problematic Fossils. Cambridge University Press, Cambridge, pp. 179–187.

Hou, X.-G., Chen, J.-Y., Lu, H.-Z., 1989. Early Cambrian new arthropods from Chengjiang, Yunan. Acta Palaeont. Sin. 28, 42–57.

Humphreys, W.F., 1993. Stygofauna in semi-arid tropical Western Australia: a Tethyan connection? Mém. Biospéol. 20, 111–116.

Koenemann, S., Iliffe, T.M., van der Ham, J., 2003. Three new species of remipede crustaceans (Speleonectidae) from Great Exuma, Bahamas Islands. Smithson. Contrib. Zool. 72, 227–252.

Koenemann, S., Iliffe, T.M., Yager, J., 2004. *Kaloketos pilosus*, a new genus and species of Remipedia (Crustacea) from the Turks and Caicos Islands. Zootaxa 618, 1–12.

Koenemann, S., Iliffe, T.M., van der Ham, J., 2007. Micropacteridae, a new family of Remipedia (Crustacea) from the Turks and Caicos Islands. Org. Divers. Evol. 7, 52–54.

Koenemann, S., Schram, F.R., Iliffe, T.M., 2006. Trunk segmentation patterns in Remipedia. Crustaceana 79, 607–631.

Schram, F.R., 1983. Remipedia and crustacean phylogeny. Crust. Issues 1, 23–28.

Schram, F.R., Hof, C.H.J., 1997. Fossils and the interrelationships of major crustacean groups. In: Edgecombe, G. (Ed.), Arthropod Fossils and Phylogeny. Columbia University Press, New York, pp. 233–302.

Schram, F.R., Koenemann, S., 2004. Shrimp cocktail: are crustaceans monophyletic? In: Cracraft, J., Donaghue, M.J. (Eds.), Assembling the Tree of Life. Oxford University Press, Oxford, New York, pp. 319–329.

Schram, F.R., Yager, J., Emerson, M.J., 1986. Remipedia. Part I. Systematics. Mem. San Diego Soc. Nat. Hist. 15, 1–60.

Yager, J., 1981. A new class of Crustacea from a marine cave in the Bahamas. J. Crust. Biol. 1, 328–333.

Yager, J., 1987a. *Cryptocorynetes haptodiscus*, new genus, new species, and *Speleonectes benjamini*, new species, of remipede crustaceans from anchialine caves in the Bahamas, with remarks on distribution and ecology. Proc. Biol. Soc. Wash. 100, 302–320.

Yager, J., 1987b. *Speleonectes tulumensis*, n. sp. (Crustacea, Remipedia) from two anchialine cenotes of the Yucatan Peninsula, Mexico. Stygologia 3, 160–166.

Yager, J., 1989. *Pleomothra apletocheles* and *Godzilliognomus frondosus*, two new genera and species of remipede crustaceans (Godzilliidae) from anchialine caves of the Bahamas. Bull. Mar. Sci. 44, 1195–1206.

Yager, J., 1994. *Speleonectes gironensis*, new species (Remipedia: Speleonectidae) from anchialine caves in Cuba, with remarks on biogeography and ecology. J. Crust. Biol. 14, 752–762.

Yager, J., Carpenter, J.H., 1999. *Speleonectes epilimnius* new species (Remipedia, Speleonectidae) from surface waters of an anchialine cave on San Salvador Island, Bahamas. Crustaceana 72, 965–977.

Yager, J., Humphreys, W.F., 1996. *Lasionectes exleyi*, sp. nov., the first remipede crustacean recorded from Australia and the Indian Ocean, with a key to the world species. Invertebr. Taxon. 10, 171–187.

Yager, J., Schram, F.R., 1986. *Lasionectes entrichoma*, n. gen., n. sp. (Crustacea, Remipedia) from anchialine caves in the Turks and Caicos, B.W.I. Proc. Biol. Wash. Soc. 99, 65–70.